PREPARED FOR THE U.S. DEPARTMENT OF ENERGY,
UNDER CONTRACT DE-AC02-76-CHO-3073

PPPL-2814
UC-427

PPPL-2814

MHD THEORY OF FIELD LINE RESONANCE IN THE MAGNETOSPHERE

BY

C.Z. CHENG, T.C. CHANG, C.A. LIN AND W.H. TSAI

January 1992

PPPL PRINCETON PLASMA PHYSICS LABORATORY

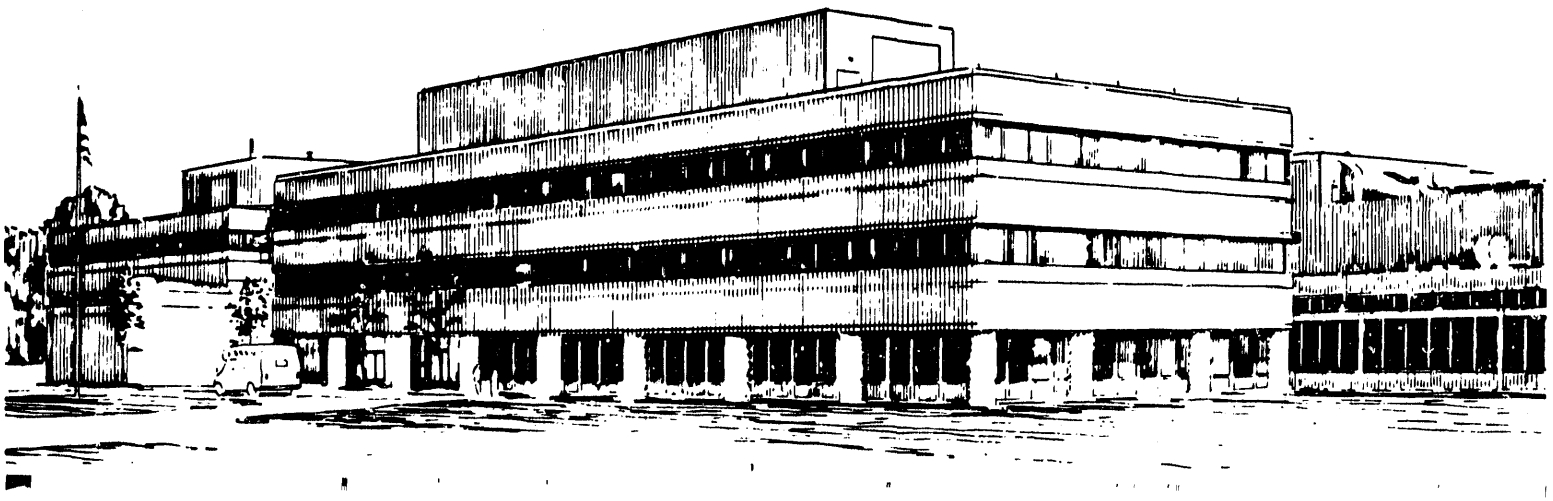

NOTICE

NOTICE

PPPL--2814

DE92 006653

MHD Theory of Field Line Resonance in the Magnetosphere

C. Z. Cheng

Princeton Plasma Physics Laboratory
Princeton University, Princeton, NJ 08543

T. C. Chang, C. A. Lin, and W. H. Tsai
Institute of Space Science
National Central University, Taiwan, ROC

Abstract

The linearized ideal MHD equations are cast into a set of global differential equations from which the field line resonance equations of the shear Alfvén waves and slow magnetosonic waves are naturally obtained for finite pressure plasmas in general magnetic field geometries with flux surfaces. The coupling between the shear Alfvén waves and the magnetosonic waves is through the geodesic magnetic field curvature. For axisymmetric magnetospheric equilibria, there is no coupling between the shear Alfvén waves and slow magnetosonic waves because the geodesic magnetic field curvature vanishes. The asymptotic singular solutions of the MHD equations near the field line resonant surface are derived. Numerical solutions of the field line resonance equations are performed for the dipole magnetic field, and it is found that the shear Alfvén wave field line resonant frequency is proportional to $L^{-4}\rho^{-1/2}$. The slow magnetosonic wave resonant frequency is much smaller than the Shear Alfvén wave resonant frequency and is roughly proportional to $P/\rho L^2$, where L is the equatorial L-shell distance, P is the plasma pressure, and ρ is the plasma mass density. The results help to understand the continuous spectra observed by AMPTE/CCE.

1. Introduction

Observations and theories of ULF magnetic pulsations have been studied for more than two decades since they were first reported in the 1960's [Judge and Coleman, 1962]. The magnetic pulsations have been classified through their frequencies, waveforms, dominant magnetic components (transverse or compressional waves), and the associated plasma and geomagnetic conditions. These morphological features provide clues for understanding their excitation mechanisms (internally-driven instabilities or externally-driven Alfvén waves). To understand the physics of the magnetic pulsations, it is most important to identify their excitation mechanisms. The internally driven plasma instabilities usually have large azimuthal mode numbers on the order of 100 and are mainly observed in the magnetosphere by satellites [Takahashi, 1988a]. The externally excited Pc waves have azimuthal polarization and small azimuthal mode numbers on the order 10 or less and is observable on the ground.

Recently, AMPTE/CCE has observed multiharmonic Alfvén resonances previously observed near geostationary orbit [Takahashi et al., 1982; Cahill et al., 1986] and firmly established that they are the most commonly excited Pc 3-5 waves in the dayside magnetosphere from the plasmapause to the magnetopause [Engebretson et al., 1986]. The distinctive structures in the azimuthal component, consisting of several frequency components, corresponds to the fundamental and the harmonics of the local toroidal Alfvén resonances. The L-shell dependence of the frequency and the latitudinal dependence of wave amplitude are unambiguous evidence for local Alfvén field line resonances.

The excitation mechanism of these pulsations has also been observed to be due to external sources. Correlating the CCE magnetic field data with simultaneous solar wind data from AMPTE/IRM, Engebretson et al. [1987] found that both the direction of the interplanetary magnetic field and the velocity of the solar wind govern the amplitude of the harmonically structured pulsations. A comprehensive statistical study of the resonant harmonic waves [Anderson et al., 1987] concluded that different source mechanisms can generate different harmonic modes at different local times. The dayside source may be related to the bow-shock-associated upstream waves, and the flankside strong fundamental waves may be driven by the Kelvin-Helmholtz instability generated waves. These toroidal Alfvén resonances can also be excited impulsively by a dayside pressure change imbedded in the solar wind [Potemra et al., 1989]

The theory of local field-line resonances of standing shear Alfvén waves in response to the propagation of external disturbances [Dungey et al., 1955; Radoski, 1966; Cummings et al., 1969; Tataronis and Grossmann, 1973; Chen and Hasegawa, 1974; Southwood, 1974] had received earlier attentions and seemed to be able to explain the basic features of low- to mid- frequency (Pc 3-5) transverse waves. The original theory of the field line resonance was studied using cold plasma model and assumed one-dimensional inhomogeneity perpendicular to the ambient magnetic field. The corresponding eigenfrequencies for the transverse shear Alfvén waves standing along the field lines also vary spatially and constitutes the so-called shear Alfvén continuum. For an excitation frequency matching an eigenfrequency inside the shear Alfvén continuum, the the wave resonance generates perturbations that are radially singular near the particular resonant magnetic field surface.

In realistic plasmas, such as the magnetospheres, besides being nonuniform in the radial direction the Alfvén velocity is also nonuniform in the azimuthal direction as well as in the direction along the ambient magnetic field, the plasma pressure is finite, and the particles are trapped in the low magnetic field region. Based on the cold plasma model, Southwood and Kivelson [1986] employed the rectangular box model to investigate the effects of parallel inhomogeneity. Chen and Cowley [1989] studied the field line resonance theory in the dipole magnetic field geometry with the cold plasma model. Lee and Lysak [1990] studied the field line resonance phenomena by solving the MHD cold plasma equations as an initial value problem. By employing the ideal MHD model with finite plasma pressure, the theory of continuous and discrete shear Alfvén spectra in toroidal plasmas has been studied [Cheng and Chance, 1986].

In the paper, we first formulate in Section 2 the ideal MHD eigenmode equations in a form to provide for a better physical representation of the MHD continuous spectra for finite pressure plasmas in general magnetic field geometries with magnetic flux surfaces. In Section 3 the field line resonances that correspond to two branches (shear Alfvén waves and slow magnetosonic waves) of the MHD continuous spectra are naturally defined [Cheng and Chance, 1986]. These two branches couple through the geodesic magnetic field curvature. In Section 4 we present asymptotic singular solutions of the MHD equations near the field line resonant surface. In Section 5 the shear Alfvén and slow magnetosonic continuous spectra are numerically studied for a dipole field geometry, and the corresponding eigenfunctions are given. The shear Alfvén wave field line resonant frequency is proportional to $L^{-4}\rho^{-1/2}$, and the slow magnetosonic wave resonant frequency is roughly proportional to $P/\rho L^2$, where L is the equatorial L-shell distance, P is the plasma pressure, and ρ is the plasma mass density. The results help to understand the continuous spectra observed by AMPTE/CCE. Finally, in Section 6 a summary of the major results is given,

and the implications of physical effects that are absent in the MHD model and the future efforts involving global computation of wave propagation are discussed.

2. MHD Eigenmode Equations

We consider static magnetospheric equilibria described by the system of equations

$$\vec{J} \times \vec{B} = \nabla P, \quad \nabla \times \vec{B} = \vec{J}, \text{ and } \nabla \bullet \vec{B} = 0, \tag{2.1}$$

where $\vec{J}$, $\vec{B}$, and P are the equilibrium current, magnetic field, and plasma pressure, respectively. For a general three dimensional magnetospheric equilibrium with nested flux surfaces, the magnetic field can be expressed as

$$\vec{B} = \nabla\psi \times \nabla\alpha, \tag{2.2}$$

where ψ is chosen as the magnetic flux function . Both ψ and α are constant along magnetic field lines. The lines where surfaces of constant ψ and constant α intersect represent magnetic field lines. Note that ψ must be a periodic function of toroidal angle ϕ in cylindrical (R, ϕ, Z) coordinate to ensure periodicity constraint. In terms of a flux coordinate system (ψ,ϕ,χ) with χ is a generalized poloidal angle varying between 0 and 2π, α can be expressed as $\alpha = \phi - q(\psi)\,\chi - \delta(\psi,\phi,\chi)$ without loss of generality, where $\delta(\psi,\phi,\chi)$ is periodic in both χ and ϕ. Note that since $\vec{B}\bullet\nabla P = 0$, P is a function of ψ only.

With the time dependence $\vec{\xi}(\vec{x},t) = \vec{\xi}(\vec{x})\exp(-i\omega t)$ and applying the Laplace transform, the linearized ideal MHD equations governing the asymptotic behaviors of the perturbed quantities are given by

$$\omega^2 \rho\, \vec{\xi} = \nabla\delta p + \vec{b} \times (\nabla \times \vec{B}) + \vec{B} \times (\nabla \times \vec{b}), \tag{2.3}$$

$$\delta p + \vec{\xi} \bullet \nabla P + \Gamma_s P\, \nabla \bullet \vec{\xi} = 0, \tag{2.4}$$

$$\vec{b} = \nabla \times (\vec{\xi} \times \vec{B}), \tag{2.5}$$

and

$$\delta\vec{E} = i\omega\,\vec{\xi}\times\vec{B}\,, \tag{2.6}$$

where $\vec{\xi}$ is the usual fluid displacement vector, $\vec{b}$ is the perturbed magnetic field, δp is the perturbed plasma pressure, and ρ is the total plasma mass density, $\delta\vec{E}$ is the perturbed electric field, and $\Gamma_s = 5/3$ is the ratio of specific heat.

We decompose the displacement vector and perturbed magnetic field as

$$\vec{\xi} = \frac{\xi_\psi \nabla\psi}{|\nabla\psi|^2} + \frac{\xi_s(\vec{B}\times\nabla\psi)}{B^2} + \frac{\xi_b\vec{B}}{B^2}\,, \tag{2.7}$$

and

$$\vec{b} = \frac{Q_\psi \nabla\psi}{|\nabla\psi|^2} + \frac{Q_s(\vec{B}\times\nabla\psi)}{|\nabla\psi|^2} + \frac{Q_b\vec{B}}{B^2}\,, \tag{2.8}$$

so that $\xi_\psi = \vec{\xi}\bullet\nabla\psi$, $\xi_s = \vec{\xi}\bullet(\vec{B}\times\nabla\psi/|\nabla\psi|^2)$, $\xi_b = \vec{\xi}\bullet\vec{B}$, $Q_\psi = \vec{b}\bullet\nabla\psi$, $Q_s = \vec{b}\bullet(\vec{B}\times\nabla\psi/B^2)$, and $Q_b = \vec{b}\bullet\vec{B}$. The three components of the induction equation, Eq. (2.5), obtained after taking the scalar products with $\nabla\psi$, $(\vec{B}\times\nabla\psi)$, and $\vec{B}$, can be written as

$$Q_\psi = \vec{B}\bullet\nabla\,\xi_\psi\,, \tag{2.9}$$

$$Q_s = \frac{|\nabla\psi|^2}{B^2}\left(\vec{B}\bullet\nabla\,\xi_s + \mathbf{S}\xi_\psi\right), \tag{2.10}$$

$$Q_b = -B^2\nabla\bullet\vec{\xi}_\perp - \vec{\xi}_\perp\bullet\nabla(P+B^2)\,, \tag{2.11}$$

where $\mathbf{S} = -(\vec{B}\times\nabla\psi/|\nabla\psi|^2)\bullet\nabla(\vec{B}\times\nabla\psi/|\nabla\psi|^2)$ is the local magnetic shear. Similarly, the three components of the momentum equation, Eq. (2.3), can be rewritten as

$$- \left(|\nabla\psi|^2 S + \vec{J} \cdot \vec{B} \right) \frac{|\nabla\psi|^2}{B^2} \left(\vec{B} \cdot \nabla \xi_s + S \xi_\psi \right) + 2 \vec{\kappa} \cdot \nabla\psi \; Q_b \, , \tag{2.12}$$

$$(\vec{B} \times \nabla\psi) \cdot \nabla \delta p_1 = \omega^2 \rho |\nabla\psi|^2 \xi_s + (\vec{B} \cdot \vec{J}) \vec{B} \cdot \nabla \xi_\psi + B^2 \vec{B} \cdot \nabla \left[\frac{|\nabla\psi|^2}{B^2} \left(\vec{B} \cdot \nabla \xi_s + S \xi_\psi \right) \right] - \nabla \cdot \left(\frac{\vec{B} \times \nabla\psi}{B^2} \right) Q_b \, , \tag{2.13}$$

$$\vec{B} \cdot \nabla \delta p_1 = \omega^2 \rho \, \xi_b - \vec{b} \cdot \nabla P \, , \tag{2.14}$$

where $\vec{\kappa} = (\vec{B}/B) \cdot \nabla (\vec{B}/B)$ is the magnetic field curvature, and δp_1 is the total perturbed pressure given by $\delta p_1 = \delta p + Q_b$.

$\nabla \cdot \vec{\xi}$ can be explicitly expressed as

$$\nabla \cdot \vec{\xi} = \frac{\nabla\psi \cdot \nabla \xi_\psi}{|\nabla\psi|^2} + \nabla \cdot \left(\frac{\nabla\psi}{|\nabla\psi|^2} \right) \xi_\psi + \vec{B} \cdot \nabla \left(\frac{\xi_b}{B^2} \right) + \frac{\vec{B} \times \nabla\psi}{B^2} \cdot \nabla \xi_s + \nabla \cdot \left(\frac{\vec{B} \times \nabla\psi}{B^2} \right) \xi_s \, . \tag{2.15}$$

Now ξ_b, Q_ψ, Q_s, and Q_b can be eliminated by using Eqs. (2.9), (2.10), and (2.14). Then after some algebra, we obtain from Eqs. (2.3) and (2.4) the following set of two-dimensional eigenmode equations [Cheng and Chance, 1986]:

$$\nabla\psi \cdot \nabla \delta p_1 = \left\{ \omega^2 \rho \, \xi_\psi + |\nabla\psi|^2 \vec{B} \cdot \nabla \left(\frac{\vec{B} \cdot \nabla \xi_\psi}{|\nabla\psi|^2} \right) - \left(|\nabla\psi|^2 S + \vec{J} \cdot \vec{B} \right) \frac{S |\nabla\psi|^2}{B^2} \xi_\psi + 2 P' K_\psi \xi_\psi \right\} + 2 K_\psi \delta p_1$$

$$- \left(|\nabla\psi|^2 \mathbf{S} + \vec{\mathbf{J}} \bullet \vec{\mathbf{B}} \right) \frac{|\nabla\psi|^2}{B^2} \vec{\mathbf{B}} \bullet \nabla \xi_s + 2\Gamma_s P K_\psi \nabla \bullet \vec{\xi} \,, \tag{2.16}$$

$$\nabla\psi \bullet \nabla\xi_\psi = - |\nabla\psi|^2 \nabla \bullet \left(\frac{\nabla\psi}{|\nabla\psi|^2} \right) \xi_\psi + |\nabla\psi|^2 \left[2K_s - \frac{\vec{B} \times \nabla\psi}{B^2} \bullet \nabla \right] \xi_s$$
$$+ |\nabla\psi|^2 \left\{ \nabla \bullet \vec{\xi} + \vec{B} \bullet \nabla \left[\frac{\Gamma_s P}{\omega^2 \rho B^2} \vec{B} \bullet \nabla \left(\nabla \bullet \vec{\xi} \right) \right] \right\} , \tag{2.17}$$

$$\left[\omega^2 \rho \frac{|\nabla\psi|^2}{B^2} \xi_s + \vec{B} \bullet \nabla \left(\frac{|\nabla\psi|^2}{B^2} \vec{B} \bullet \nabla \xi_s \right) \right] + 2\Gamma_s P K_s \nabla \bullet \vec{\xi}$$
$$= - \vec{B} \bullet \nabla \left(\frac{|\nabla\psi|^2}{B^2} \mathbf{S} \, \xi_\psi \right) - 2P' K_s \xi_\psi - \left(\vec{\mathbf{J}} \bullet \vec{\mathbf{B}} \right) \vec{B} \bullet \nabla \xi_\psi$$
$$+ \left[\frac{\vec{B} \times \nabla\psi}{B^2} \bullet \nabla - 2 K_s \right] \delta p_1 \,, \tag{2.18}$$

$$\left\{ \left(1 + \frac{\Gamma_s P}{B^2} \right) \nabla \bullet \vec{\xi} + \vec{B} \bullet \nabla \left[\frac{\Gamma_s P}{\omega^2 \rho B^2} \vec{B} \bullet \nabla \left(\nabla \bullet \vec{\xi} \right) \right] \right\} + 2 K_s \xi_s$$
$$= - \left[\frac{2 K_\psi}{|\nabla\psi|^2} \right] \xi_\psi - \frac{\delta p_1}{B^2} \,, \tag{2.19}$$

where $P' = \partial P / \partial\psi$, $K_\psi = \vec{\kappa} \bullet \nabla\psi$ is the radial magnetic field curvature, and $K_S = (\vec{\kappa} \bullet \vec{B} \times \nabla\psi)/B^2$ is the geodesic magnetic field curvature. Note that from Eq.(2.4) Q_b can be expressed as

$$Q_b = \delta p_1 + P' \xi_\psi + \Gamma_s P \nabla \bullet \vec{\xi} \,. \tag{2.20}$$

Eqs. (2.16)-(2.19) represent the set of eigenmode equations describing the MHD wave propagation and MHD instabilities in a general plasma system with magnetic flux surfaces. Eqs. (2.16)-(2.19) can be written symbolically in the following form

$$\frac{\partial}{\partial\psi}\begin{pmatrix}\delta p_1\\ \xi_\psi\end{pmatrix} = C\begin{pmatrix}\delta p_1\\ \xi_\psi\end{pmatrix} + D\begin{pmatrix}\xi_s\\ \nabla\bullet\vec{\xi}\end{pmatrix}, \tag{2.22}$$

and

$$E\begin{pmatrix}\xi_s\\ \nabla\bullet\vec{\xi}\end{pmatrix} = F\begin{pmatrix}\delta p_1\\ \xi_\psi\end{pmatrix}, \tag{2.23}$$

where C, D, E, F are 2×2 matrix operators involving only surface derivatives $\vec{B}\bullet\nabla$ and $(\vec{B}\times\nabla\psi)\bullet\nabla$.

3. The Continuous Spectrum

For a given magnetospheric equilibrium, we first solve ξ_s and $\nabla\bullet\vec{\xi}$ in terms of δp_1 and ξ_ψ from Eq. (2.23) by inverting the surface matrix operator E. Eq.(2.22) then reduces to an equation for δp_1 and ξ_ψ, i.e.,

$$\frac{\partial}{\partial\psi}\begin{pmatrix}\delta p_1\\ \xi_\psi\end{pmatrix} = (C + DE^{-1}F)\begin{pmatrix}\delta p_1\\ \xi_\psi\end{pmatrix}. \tag{3.1}$$

Admissible regular solutions of Eq.(3.1) must satisfy the proper boundary conditions. This procedure fails if the inverse of the surface operator E does not exists (i.e., det|E| = 0) for a given ω_o at certain flux surface ψ_o. Then Eq.(3.1) has a radial singularity at ψ_o, and non-square-integrable solutions of ξ_ψ and δp_1 with logarithmic singularity along the ψ-direction at the singular surface ψ_o are possible.

Therefore, the MHD continuous spectrum is determined by the eigenvalues ω of the equation

$$E \begin{pmatrix} \xi_s \\ \nabla\bullet\vec{\xi} \end{pmatrix} = 0 \ , \tag{3.2}$$

on each flux surface ψ with non-trivial single-valued eigenfunctions ξ_s and $\nabla\bullet\vec{\xi}$ satisfying appropriate boundary conditions along the field line. Since Eq.(3.2) can be reduced to a fourth order ordinary differential equation along the field line with the coefficients being all non-singular, the eigenvalues ω must be discrete. Thus, at each flux surface ψ, a discrete set of eigenvalues $\omega_n(\psi)$, where n is an integer, can be found with the corresponding eigenfunctions $\xi_{s(n)}$ and $(\nabla\bullet\vec{\xi})_{(n)}$ satisfying appropriate boundary conditions along the field line. Both the eigenvalues $\omega_n(\psi)$ and eigenfunctions $\xi_{s(n)}$ and $(\nabla\bullet\vec{\xi})_{(n)}$ are smooth functions of ψ and form the discrete continuous spectra for the equilibrium. Note that $\xi_{s(n)}$ and $(\nabla\bullet\vec{\xi})_{(n)}$ are linearly dependent through Eq.(3.2).

Eq.(3.2) represents the coupling of two branches of MHD field line resonances - the shear Alfvén branch and the slow magnetosonic branch - through the geodesic magnetic field curvature K_s. We also note that in the cold plasma limit (P=0), Eq. (3.2) reduces to a second order ordinary differential equation, and the slow magnetosonic wave does not exist with corresponding eigenfunctions $(\nabla\bullet\vec{\xi})_{(n)}$ becoming trivial. As will be shown in Section 3, near the resonant surface ψ_o, ξ_ψ and δp_1 diverge logarithmically, while ξ_s and $\nabla\bullet\vec{\xi}$ diverge as $(\psi-\psi_o)^{-1}$. Thus, the dominant eigenfunctions of the shear Alfvén branch at the resonant surface are mainly in terms of ξ_s and correspondingly in the components of the radial electric field $\delta\vec{E}\bullet\nabla\psi$ and shear magnetic field $Q_s = \vec{b}\bullet(\vec{B}\times\nabla\psi/B^2)$ as seen from Eqs.(2.6) and (2.10). The dominant eigenfunctions of the slow magnetosonic branch at the resonant surface are given by the compressibility $\nabla\bullet\vec{\xi}$ and are hence from Eq.(2.20) by the compressional magnetic field Q_b. The perpendicular electromagnetic field components are smaller.

Operating on Eq.(3.2) with the matrix $[\ \xi_s\ -(\nabla\bullet\vec{\xi})]$, and integrating along the field line with ds/B, a Lagrangian functional L can be obtained and is given by

$$L = \int_{s_1}^{s_2} \frac{ds}{B} \left\{ \omega^2 \rho \left(\frac{|\nabla\psi|^2}{B^2} |\xi_s|^2 + B^2 |Z|^2 \right) \right.$$

$$- \left[\frac{|\nabla\psi|^2}{B^2} |\vec{B} \bullet \nabla \xi_s|^2 + \frac{\Gamma_s P + B^2}{\Gamma_s P B^2} |\nabla \bullet \vec{\xi}|^2 \right] \Bigg\} , \tag{3.3}$$

where s denotes the distance along the field line so that $\vec{B}\bullet\nabla = B(d/ds)$, $Z = \Gamma_s P\, \vec{B}\bullet\nabla(\nabla\bullet\vec{\xi}) / \rho\omega^2 B^2$, and s_1 and s_2 are the two end points of the field line. In deriving Eq.(3.3) we have employed the standing wave boundary conditions with ξ_s and $\nabla\bullet\vec{\xi}$ vanishing at the two end points of the field line. It is straight forward to verify that Eq. (3.2) is a consequence of the requirement that the functional L be stationary. Since $L = 0$, it is clear that the eigenvalues ω_n and the corresponding eigenfunctions must be real. The determination of the continuous spectrum reduces to that of finding the eigenvalues ω and eigenfunctions so that the Lagrangian functional L is stationary with respect to variatios of ξ_s and $\nabla\bullet\vec{\xi}$. The admissible variational functions must be square-integrable and satisfy the standing wave boundary condition.

One can also show that the discrete set of eigenfunctions $\{ \xi_{s(n)} ; (\nabla\bullet\vec{\xi})_{(n)} \}$ are complete and orthogonal with the orthogonality condition given by

$$\int_{s_1}^{s_2} \frac{ds}{B}\ \rho \left(\frac{|\nabla\psi|^2}{B^2} \xi_{s(n)} \xi_{s(n')} + B^2 Z_{(n)} Z_{(n')} \right) = \delta_{n\,n'} , \tag{3.4}$$

where $\delta_{n\,n'}$ is the Kronecker delta. It can be straight forwardly shown that

$$(\omega_n^{\,2} - \omega_{n'}^{\,2}) \int_{s_1}^{s_2} \frac{ds}{B}\ \rho \left(\frac{|\nabla\psi|^2}{B^2} \xi_{s(n)} \xi_{s(n')} + B^2 Z_{(n)} Z_{(n')} \right) = 0 , \tag{3.5}$$

from which the orthogonality condition Eq.(3.4) follows.

Thus, we have established that there are only two branches of continuous spectra in the ideal MHD theory for finite pressure plasmas in general magnetic field geometries with flux surfaces. In general there are three branches of MHD waves. The third branch of MHD waves, the fast

magnetosonic wave, represents a regular global solution of Eq.(3.1), which is influenced by the local magnetic shear, the magnetic field curvature, and the field-aligned current.

For a simplified axisymmetric magnetosphere with nested magnetic flux surfaces, the magnetic field can be expressed as

$$\vec{B} = \nabla\psi \times \nabla\phi . \tag{3.6}$$

where ψ is a function of R and Z only. Since $\vec{B}\bullet\nabla\psi = \vec{B}\bullet\nabla\phi = 0$, the lines of the magnetic field and the lines of constant ψ coincide. The local magnetic shear **S** and the field-aligned current $\vec{J}\bullet\vec{B}$ vanish. We also note that the geodesic magnetic field curvature K_S vanishes, and the shear Alfvén waves and the slow magnetosonic waves decouple as shown in Eq.(3.2). In the decoupled limit the Shear Alfvén field line resonance equation given by Eq. (3.2) corresponds to the toroidal magnetic field equation previously studied numerically by Cummings et al. [1969] by employing a model field-aligned density profile. The finite pressure effect enters through the change in the equilibrium magnetic field. In addition, to be consistent with the ideal MHD model the density should be constant along the field line. The effect of the field-aligned density variation will be considered in the future with a consistent anisotropic MHD model.

4. Singular Solutions Near Field Line Resonant Surface

To obtain the radial field structure near the field line resonant surface, we will follow the approach of Pao [1975] in his investigations of the continuous spectrum in axisymmetric tokamaks. By first assuming the existence of singular solutions of Eqs.(2.22-23) near the resonant surface, the necessary compatibility conditions are then derived. We also note that Chen and Cowley [1989] has used the similar approach to obtain the singular solutions near field line resonant surface for a cold plasma model.

Let ψ_o label the field line resonant surface of an external disturbance with the excitation frequency $\omega^2 = \omega_n^2(\psi_o)$, and we define a smallness parameter $\varepsilon = |(\psi-\psi_o)/\psi_o| << 1$. Therefore, there are two spatial scales; the slow equilibrium scale and the fast radial perturbation scale. We note the following orderings: $|\psi_o(\partial/\partial\psi)| \sim O(1/\varepsilon) >> 1$, the operator $E \sim O(\varepsilon)$, and the operators C, D, $F \sim O(1)$. Then, the solutions of Eq.(2.22-23) near the resonant surface ψ_o can be expanded asymptotically as

$$\delta p_1 = \delta p_1^{(0)} + \delta p_1^{(1)} + \ldots ,$$

$$\xi_\psi = \xi_\psi^{(0)} + \xi_\psi^{(1)} + \ldots ,$$

$$\xi_s = \xi_s^{(-1)} + \xi_s^{(0)} + \xi_s^{(1)} + \ldots ,$$

$$\nabla\bullet\vec{\xi} = (\nabla\bullet\vec{\xi})^{(-1)} + (\nabla\bullet\vec{\xi})^{(0)} + (\nabla\bullet\vec{\xi})^{(1)} + \ldots , \tag{4.1}$$

where the superscripts denote orderings in ε. Then, from Eq.(2.22) we have in the lowest order

$$\frac{\partial}{\partial\psi}\begin{pmatrix} \delta p_1^{(0)} \\ \xi_\psi^{(0)} \end{pmatrix} = D\begin{pmatrix} \xi_s^{(-1)} \\ (\nabla\bullet\vec{\xi})^{(-1)} \end{pmatrix} , \tag{4.2}$$

and from Eq.(2.23) we have

$$E\begin{pmatrix} \xi_s^{(-1)} \\ (\nabla\bullet\vec{\xi})^{(-1)} \end{pmatrix} = F\begin{pmatrix} \delta p_1^{(0)} \\ \xi_\psi^{(0)} \end{pmatrix} . \tag{4.3}$$

To proceed further we express $\xi_s^{(-1)}$ and $(\nabla\bullet\vec{\xi})^{(-1)}$ in terms of the field line resonance eigenfunctions $\xi_{s(n)}$ and $(\nabla\bullet\vec{\xi})_{(n)}$ as

$$\begin{pmatrix} \xi_s^{(-1)}(s,\psi) \\ (\nabla\bullet\vec{\xi})^{(-1)}(s,\psi) \end{pmatrix} = \sum_n \lambda_n(y,\psi)\begin{pmatrix} \xi_{s(n)}(s,\psi) \\ (\nabla\bullet\vec{\xi})_{(n)}(s,\psi) \end{pmatrix} , \tag{4.4}$$

where $y = (\psi - \psi_o)$ and ψ represent the fast and slow radial variations in ψ, respectively. Substituting Eq.(4.4) into Eq.(4.3), operating on Eq.(4.3) with the matrix $[\ \xi_{s(n)} \ -(\nabla\bullet\vec{\xi})_{(n)}\ ]$, integrating Eq.(4.3) along the field line with ds/B, and applying the orthogonality condition Eq.(3.4), we then have

$$[\omega^2 - \omega_n^2(\psi)\ ]\ \lambda_n(y,\psi) \ = \ A_n(\psi)\ , \tag{4.5}$$

where

$$A_n(\psi) \equiv \int_{s_1}^{s_2} \frac{ds}{B} \left[\ \xi_{s(n)} \ \ -(\nabla\bullet\vec{\xi})_{(n)} \right] F \begin{bmatrix} \delta p_1^{(0)} \\ \xi_\psi^{(0)} \end{bmatrix} . \tag{4.6}$$

Note that we have demanded $A_n(\psi)$ to be finite and dependent on ψ but not on y. Then, Eq.(4.5) readily shows the singular nature of $\lambda_n(y,\psi)$ near the resonant surface ψ_o where $\omega^2 = \omega_n^2(\psi_o)$; i.e.,

$$\lambda_n(y,\psi) = \frac{A_n(\psi)}{[\ \omega^2 - \omega_n^2(\psi)\ ]} \equiv \frac{f_n(\psi)}{y} . \tag{4.7}$$

Integrating Eq.(4.2) over y by making use of Eq.(4.4) and noting that $D \sim O(1)$, we have

$$\begin{bmatrix} \delta p_1^{(0)} \\ \xi_\psi^{(0)} \end{bmatrix} = \sum_n \int dy\ \lambda_n(y,\psi)\ D \begin{bmatrix} \xi_{s(n)}(s,\psi) \\ (\nabla\bullet\vec{\xi})_{(n)}(s,\psi) \end{bmatrix} + \begin{bmatrix} C_p(\psi) \\ C_\xi(\psi) \end{bmatrix}$$

$$= \ln(y)\ f_n(\psi)\ D \begin{bmatrix} \xi_{s(n)}(s,\psi) \\ (\nabla\bullet\vec{\xi})_{(n)}(s,\psi) \end{bmatrix} + \begin{bmatrix} C_p(s,\psi) \\ C_\xi(s,\psi) \end{bmatrix} , \tag{4.8}$$

where $C_p(s,\psi)$ and $C_\xi(s,\psi)$ are integration constants that depend on the slow equilibrium scale. By substituting Eq.(4.8) into Eq.(4.6), the constraint that A_n depends only on ψ but not on y can be met if the compatibility condition,

$$\int_{s_1}^{s_2} \frac{ds}{B} \left[\xi_{s(n)} \quad -(\nabla\bullet\vec{\xi})_{(n)} \right] F\, D \begin{pmatrix} \xi_{s(n)}(s,\psi) \\ (\nabla\bullet\vec{\xi})_{(n)}(s,\psi) \end{pmatrix} = 0 , \tag{4.9}$$

is satisfied.

For the cold plasma model in a dipole magnetic field [Chen and Cowley, 1989], the compatibility condition, Eq.(4.9), is trivially satisfied by noting that the geodesic magnetic field curvature K_s, field-aligned current $\vec{J}\bullet\vec{B}$, the local magnetic shear **S**, and the leading order compressibility $(\nabla\bullet\vec{\xi})^{(-1)}$, i.e., $(\nabla\bullet\vec{\xi})_{(n)}$, are all vanished. Following the analytical procedure presented in this section, it can be easily shown that δp_1, which reduces to the compressional magnetic field $\vec{b}\bullet\vec{B}$ in the cold plasma limit, is a constant in the fast y scale [Chen and Cowley, 1989]. Also from Eqs. (2.19) and (4.8) that $\nabla\bullet\vec{\xi}$ and ξ_ψ have a logarithmic singularity $\psi \rightarrow \psi_o$. On the other hand, ξ_s diverge as $(\psi-\psi_o)^{-1}$. This result is similar to that with one-dimensional nonuniformity perpendicular to the field line in the cold plasma limit[Tataronis and Grossmann, 1973; Chen and Hasegawa, 1974; Southwood, 1974].

Thus, we have shown that in the ideal MHD model with finite pressure ξ_ψ and δp_1 have a logarithmic singularity as $\psi \rightarrow \psi_o$, while ξ_s and $\nabla\bullet\vec{\xi}$ diverge as $(\psi-\psi_o)^{-1}$. We also note that for a given excitation frequency in general there can be more than one resonant surfaces. The strength of the coupling to field line resonances depends on $A_n(\psi)$, which represents the projection of the perturbations ξ_ψ and δp_1 into the field line resonance eigenfunctions $\xi_{s(n)}$ and $(\nabla\bullet\vec{\xi})_{(n)}$ at the local resonant surface ψ_o. From Eq.(2.9) ξ_ψ relates to the radial magnetic field perturbation, and δp_1 corresponds to the parallel magnetic field perturbation in the cold plasma limit.

5. The Continuous Spectrum in a Dipole Magnetic Field

In the following we will present solutions of the field line resonances for the shear Alfvén and slow magnetospheric continuum in a dipole magnetic field geometry. For the dipole magnetic field we have $\psi = -M\cos^2\theta / r$, where r and θ are the radius and polar angle in a right-handed spherical coordinate system (r,θ,ϕ) with $-\pi/2 \le \theta \le \pi/2$, and M is the dipole moment. The components of the dipole magnetic field are given by $B_r = 2M\sin\theta / r^3$, and $B_\theta = -M\cos\theta /$

r^3. In terms of the (ψ,θ,ϕ) flux coordinate system the Jacobian is $J = (\nabla\psi\times\nabla\theta\bullet\nabla\phi)^{-1} = r^4 / M\cos\theta$, and $\vec{B}\bullet\nabla = -J^{-1}(\partial/\partial\vartheta)$ on a flux surface. To be consistent with the ideal MHD model we have taken both the plasma density and pressure to be constant along the field line. The shear Alfvén waves and the slow magnetosonic waves decouple, and their governing field line resonance equations, Eq.(3.2), are given independently. The shear Alfvén resonance equation is given in a dimensionless form by

$$\frac{d}{d\theta}\left[(\cos\theta)^{-1}\frac{d\xi_s}{d\theta}\right] + \Omega^2\cos^{13}\theta\,\xi_s = 0, \tag{5.1}$$

where $\Omega^2 = (\omega L/v_A)^2$, $v_A^2 = B_o^2/\rho$ is the square of the Alfvén speed at the equator, $B_o(L) = M/L^3$ is the dipole magnetic field intensity at the equator, and L is the equatorial L-shell distance. Note that numerical solutions of the shear Alfvén resonance equation with a model density profile along the field line had been studied by Cummings et al. [1969]. Similarly, the slow magnetosonic resonance equation is given in a dimensionless form by

$$\frac{d}{d\theta}\left[\frac{\beta\cos^5\theta}{(1+3\sin^2\theta)}\frac{d}{d\theta}\nabla\bullet\vec{\xi}\right] + \Omega^2\cos^7\theta\left[1+\frac{\beta\cos^{12}\theta}{(1+3\sin^2\theta)}\right]\nabla\bullet\vec{\xi} = 0, \tag{5.2}$$

where $\beta = \Gamma_s P/B_o^2$ is the plasma beta at the equator. Then, Eqs.(5.1) and (5.2) are solved numerically by a shooting method with the reflecting boundary conditions that the perturbations vanish on the Earth's surface for each field line. Note from Eqs. (5.1) and (5.2) that for different L-shells the dimensionless eigenvalues Ω for the shear Alfvén wave depend only on the boundary condition through the boundary θ locations, and the dimensionless eigenvalues Ω for the slow magnetosonic wave depend on both the equatorial plasma beta and the boundary θ locations.

Table 1 shows the eigenvalues Ω_n^2 of the shear Alfvén resonances versus L values ranging from 3 to $10R_E$ for three symmetric and three antisymmetric modes, where n represents the number of points the corresponding eigenfunction goes through zero excluding the boundary points. It is clear that the eigenvalues Ω_n^2 are fairly constant versus L, and we conclude that the shear Alfvén resonant frequency ω is proportional to $L^{-4}\rho^{-1/2}$. If we assume that the plasma density is proportional to L^{-k}, then $\omega \propto L^{k/2-4}$. Since k is usually near 4 [Chappell, 1974; Poulter et al., 1984], we have $\omega \propto L^{-2}$. At L=6 resonant surface the field-aligned shear Alfvén wave eigenfunctions of three lowest symmetric modes (n = 0, 2, 4) and three lowest antisymmetric

modes (n = 1, 3, 5) versus θ are shown in Fig. 1. Fig. 1(a) shows the toroidal fluid displacement ξ_s, Fig. 1(b) shows the corresponding toroidal perturbed magnetic field $b_\phi = \vec{b}\bullet\nabla\phi/|\nabla\phi|$, and Fig. 1(c) shows the corresponding radial electric field $i\delta E_\psi = i\delta\vec{E}\bullet\nabla\psi/|\nabla\psi|$. In calculating b_ϕ and δE_ψ we have made use of the relations Eqs. (2.10) and (2.6) by noting that the local magnetic shear **S** vanishes for axisymmetric magnetospheric equilibrium.

Table 2 shows the eigenvalues Ω_n^2 of the slow magnetosonic resonances versus L values ranging from 3 to $10R_E$ for three symmetric and three antisymmetric modes, where n represents the number of points the corresponding eigenfunction goes through zero excluding the boundary points. The equatorial beta values β versus L are chosen to represent realistic magnetospheric condition. It is clear that the eigenvalues Ω_n^2 are roughly proportional to β, and we conclude that for $\beta < 1$ the slow magnetosonic wave resonant frequency ω is roughly proportional to $P/\rho L^2$. Note that the slow magnetosonic wave eigenfrequencies are much smaller than the corresponding shear Alfvén wave eigenfrequencies. The dominant eigenfunction $\nabla\bullet\vec{\xi}$ of the slow magnetosonic wave at the L=6 resonant surface for three lowest symmetric modes (n = 0, 2, 4) and three lowest antisymmetric modes (n = 1, 3, 5) versus θ are shown in Fig. 2.

6. Summary and Discussions

In the paper we have shown analytically that in the frame work of ideal MHD model field line resonances of standing shear Alfvén and slow magnetosonic waves exist in a general magnetic field geometries with flux surfaces. These two branches of continuous spectra couple through the geodesic magnetic field curvature. The theoretically predicted wave properties near the resonant surfaces are similar to those of the previous one-dimensional model, but the field-aligned wave structures are given by the field line resonance eigenfunctions $\{\xi_{s(n)}\,;\,(\nabla\bullet\vec{\xi})_{(n)}\}$ with corresponding eigenfrequencies $\{\omega_n\}$. The continuous spectra (eigenfrequencies and corresponding eigenfunctions) of the shear Alfvén waves and the slow magnetosonic waves are numerically obtained in a dipole magnetic field. We find that the shear Alfvén resonant frequency ω is proportional to $L^{-4}\rho^{-1/2}$ and the slow magnetosonic wave resonant frequency ω is roughly proportional to $P/\rho L^2$. Typically, the slow magnetosonic wave frequencies are smaller than those of shear Alfvén waves with similar nodal structures even for equatorial beta value in the order of unity. The harmonically structured continuous spectrum of the azimuthal magnetic field oscillations as a function of L shell observed by AMPTE/CCE [Engebretson et al., 1986] can be

reasonably interpreted by the shear Alfvén resonant frequency scaling of $L^{-4}\rho^{-1/2}$. No observational evidence has been established for the slow magnetosonic continuous spectrum in the magnetosphere. This may be related to the fact that the slow magnetosonic resonant frequencies are much smaller than the shear Alfvén resonant frequencies and thus less likely to be observed by the fast flying satellite. Another possibility may be because the slow magnetosonic waves are easily Landau damped if ion temperature is roughly equal or larger than electron temperature as is usually the case in the magnetosphere. It is usually difficult to extract small amplitude oscillations.

The question of the coupling between the global compressional pulsations with the local standing Alfvén resonance [Kivelson and Southwood, 1985] has been examined by Engebretson et al. [1986] and Takahashi et al. [1988b]. Engebretson et al. [1986] concluded that there was no evidence of the global mode with frequency remaining constant across L shells in the dynamic spectra of the CCE magnetic field data. Takahashi et al. [1988b] reported a coexistence of a compressional magnetic pulsation and a toroidal Alfvén resonance. However, they concluded that these two waves do not couple because of frequency mismatch, and suggested that the toroidal resonances represent transient oscillations caused by external pressure variations. In order to have a better theoretical understanding of this issue, we have to solve the global MHD equations, Eqs. (2.22-23), to obtain the global wave propagation property. By imposing a source disturbance at the magnetopause boundary as a boundary condition, one can obtain the L-shell dependence of the field line resonance power spectrum. Thus, a global MHD solution will not only provide the information of radial wave structures, but also improve our understanding of the azimuthal asymmetry of the field line resonances.

The field line resonances and the global radial wave structures can be studied by employing a self-consistent magnetospheric equilibrium with anisotropic pressure [Cheng, 1991a] to understand the finite plasma pressure and pressure anisotropy effects. A proper formulation for anisotropic pressure is under development. Furthermore, implications due to particle trapping and other kinetic effects [Cheng, 1991b] will be studied in the future.

Acknowledgment

This work is supported by NSF Grant No. ATM-8911638 and DoE Contract No. DE-AC02-76-CHO3073 at Princeton University and by the National Science Council of the Republic of China under grant NSC 80-0202-M008-14 at National Central University.

References

Allan, W., S. P. White, and E. M. Poulter, Impulse-excited hydromagnetic cavity and field-line resonances in the magnetosphere, Planet. Space Sci., 34, 371, 1986.

Anderson, B. J., M. J. Engebretson, L. J. Zanetti, and T. A. Potemra, A statistical study of Pc 3-5 pulsations observed by the AMPTE/CCE spacecraft magnetic filed experiments: Evidence for distinct dayside and flank excitation mechanisms, in Proceedings of the 1987 Cambridge Workshop in Theoretical Geoplasma Physics, MIT, July 28-Aug. 1., 1987.

Cahill, L. J., Jr., Lin, N. G., Engebretson, M. J., Weimer, D. R., and Sugiura, M., Electric and magnetic observations of the structure of standing waves in the magnetosphere, J. Geophys. Res., 91, 8895, 1986.Chen, L., and A. Hasegawa, A theory of long-period magnetic pulsations, J. Geophys. Res., 79, 1024, 1974.

Chappell, C. R., Detached plasma regions in the magnetosphere, J. Geophys. Res., 79, 1861, 1974.

Chen, L., and A. Hasegawa, A theory of long-period magnetic pulsations, 1. Steady state excitation of field line resonances, J. Geophys. Res., 79, 1024, 1974.

Chen, L., and S. C. Cowley, On field line resonances of hydromagnetic Alfvén waves in dipole magnetic field, Geophys. Res. Lett., 16, 895, 1989.

Cheng, C. Z., and M. S. Chance, Low-n shear Alfvén spectra in axisymmetric toroidal plasmas, Phys. Fluids, 29, 3695, 1986.

Cheng, C. Z., Magnetospheric equilibrium with anisotropic pressure, Princeton Plasma Physics Laboratory Report PPPL- 2762, to appear in J. Geophys. Res., 1991a.

Cheng, C. Z., A kinetic-MHD model for low frequency phenomena, Princeton Plasma Physics Laboratory Report PPPL- 2766, to appear in J. Geophys. Res., 1991b.

Cummings, W. D., R. J. O'Sullivan, and P. J. Coleman, Jr., Standing Alfvén waves in the magnetosphere, J. Geophys. Res., 74, 778, 1969.

Engebretson, M. J., L. J. Zanetti, T. A. Potemra, and M. H. Acuna, Harmonically structured ULF pulsations observed by the AMPTE CCE magnetic field experiment, Geophys. Res. Lett., 13, 905, 1986.

Engebretson, M. J., L. J. Zanetti, T. A. Potemra, W. Baumjohann, and H. Luhr, Simultaneous observations of Pc 3-4 pulsations in the solar wind and in the Earth's magnetosphere, J. Geophys. Res., 92,10053, 1987.

Judge, D. L., and P. J. Coleman, Jr., Observations of low-frequency hydromagnetic waves in the distant geomagnetic field, Explorer 6, J. Geophys. Res., 67, 5071, 1962.

Lee, D. H., and R. L. Lysak, Effects of azimuthal asymmetry on ULF waves in the dipole magnetosphere, Geophys. Res. Lett., 17, 53, 1990.

Pao, Y. P., The continuous spectrum in toroidal geometries, Nucl. Fusion, 15, 631, 1975.

Potemra, T. A., L. J. Zanetti, and M. H. Acuna, The AMPTE CCE magnetic field experiment, IEEE Trans. Geosci. Remote Sen., GE-23, 246-249, 1985.

Potemra, T. A., H. Luhr, L. J. Zanetti, K. Takahashi, R. E. Erlandson, G. T. Marklund, L. P. Block, L. G. Bloomberg, and R. P. Lepping, Multi-satellite and ground-based observations of transient ULF waves, J. Geophys. Res., 94, 2543, 1989.

Poulter, E. M., W. Allan, J. G. Keys, and E. Nielsen, Plasmatrough ion mass densities determined from ULF pulsation eigenperiods, Planet. Space Sci., 32, 1069, 1984.

Radoski, H. R., Magnetic toroidal resonances and vibrating field lines, J. Geophys. Res., 71, 1891, 1966.

Sonnerup, B. U. O., L. J. Cahill, Jr., and L. R. Davis, Resonant vibration of the magnetosphere observed from Explorer 26, J. Geophys. Res., 74, 2276, 1969.

Southwood, D. J., Some features of field line resonances in the magnetosphere, Planet. Space Sci. 22, 483, 1974.

Southwood, D. J., and M. G. Kivelson, The effect of parallel inhomogeneity on magnetospheric wave coupling, J. Geophys. Res., 91, 6871, 1986.

Takahashi, K., and McPherron, R. L., Harmonic structure of Pc 3-4 pulsations, J. Geophys. Res., 87, 1504, 1982.

Takahashi, K., Multisatellite studies of ULF waves, Advance in Space Res., 8, 427,1988a.

Takahashi, K., L. M. Kistler, T. A. Potemra, R. W. McEntire, and L. J. Zanetti, Magnetospheric ULF waves observed during the major magnetospheric compression of November 1, 1984, J. Geophys. Res., 93, 14369, 1988b.

Tataronis, J., and W. Grossmann, Decay of MHD waves by phase mixing, I, The sheet pinch in plane geometry, Z. Phys. 261, 203, 1973.

Figure Captions

Fig. 1. The field-aligned structures of shear Alfvén wave eigenfunctions, (a) the toroidal fluid displacement ξ_s, (b) the corresponding toroidal perturbed magnetic field $b_\phi = \vec{b}\bullet\nabla\phi/|\nabla\phi|$, and (c) the corresponding radial electric field $i\delta E_\psi = i\delta\vec{E}\bullet\nabla\psi/|\nabla\psi|$, of three lowest symmetric modes (n=0, 2, 4) and three lowest antisymmetric modes (n=1, 3, 5). The eigenfunctions are evaluated at L=6.

Fig. 2. The field-aligned structures of slow magnetosonic wave eigenfunctions, $\nabla\bullet\vec{\xi}$, of three lowest symmetric modes (n=0, 2, 4) and three lowest antisymmetric modes (n=1, 3, 5). The eigenfunctions are evaluated at L=6.

TABLE 1. Eigenfrequencies of Shear Alfvén Waves

L	Ω^2 (n=0)	Ω^2 (n=1)	Ω^2 (n=2)	Ω^2 (n=3)	Ω^2 (n=4)	Ω^2 (n=5)
3	5.0	33.1	85.5	161.9	262.2	386.4
4	4.7	32.2	83.7	159.0	258.0	380.7
5	4.6	32.0	83.3	158.5	257.5	380.3
6	4.5	31.5	82.3	156.9	255.1	376.9
7	4.4	31.3	81.9	156.3	254.2	375.8
8	4.4	31.1	81.6	155.8	253.6	375.0
9	4.4	31.2	81.9	156.3	254.5	375.4
10	4.3	31.1	81.7	156.0	254.1	375.9

TABLE 2. Eigenfrequencies of Slow Magnetosonic Waves

L	β	Ω^2 (n=0)	Ω^2 (n=1)	Ω^2 (n=2)	Ω^2 (n=3)	Ω^2 (n=4)	Ω^2 (n=5)
3	0.139	0.021	1.1	2.4	4.2	6.6	9.5
4	0.221	0.020	1.7	3.5	6.2	9.5	13.6
5	0.315	0.018	2.3	4.7	8.3	12.8	18.2
6	0.452	0.016	2.8	5.7	10.0	15.3	21.8
7	0.590	0.016	3.9	8.1	14.0	21.5	30.5
8	0.5	0.011	3.4	6.9	11.9	18.3	25.9
9	0.450	0.008	3.0	6.2	10.8	16.5	23.3
10	0.398	0.006	2.7	5.5	9.6	9.6	20.7

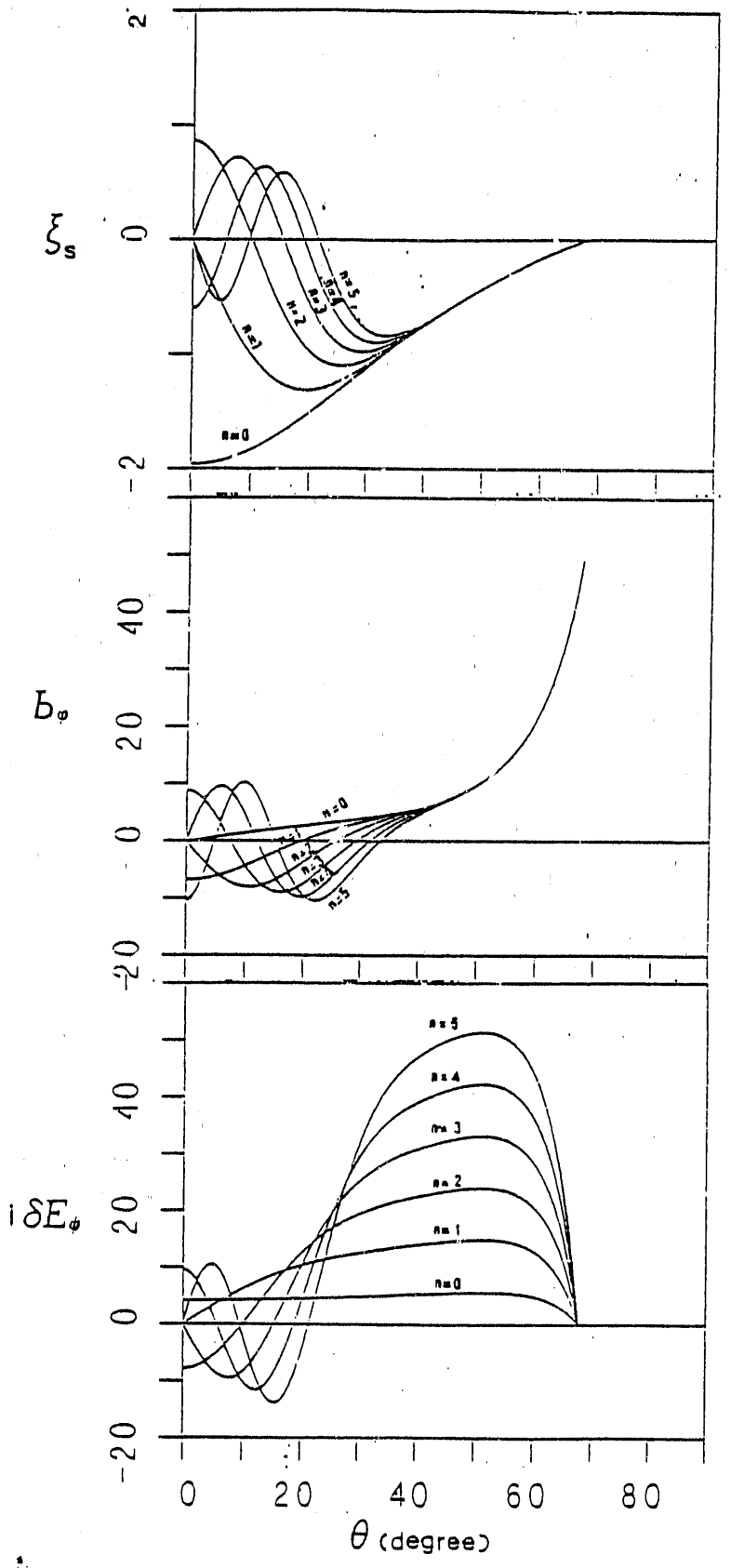

Fig. 1 Shear Alfvén Waves (L=6)

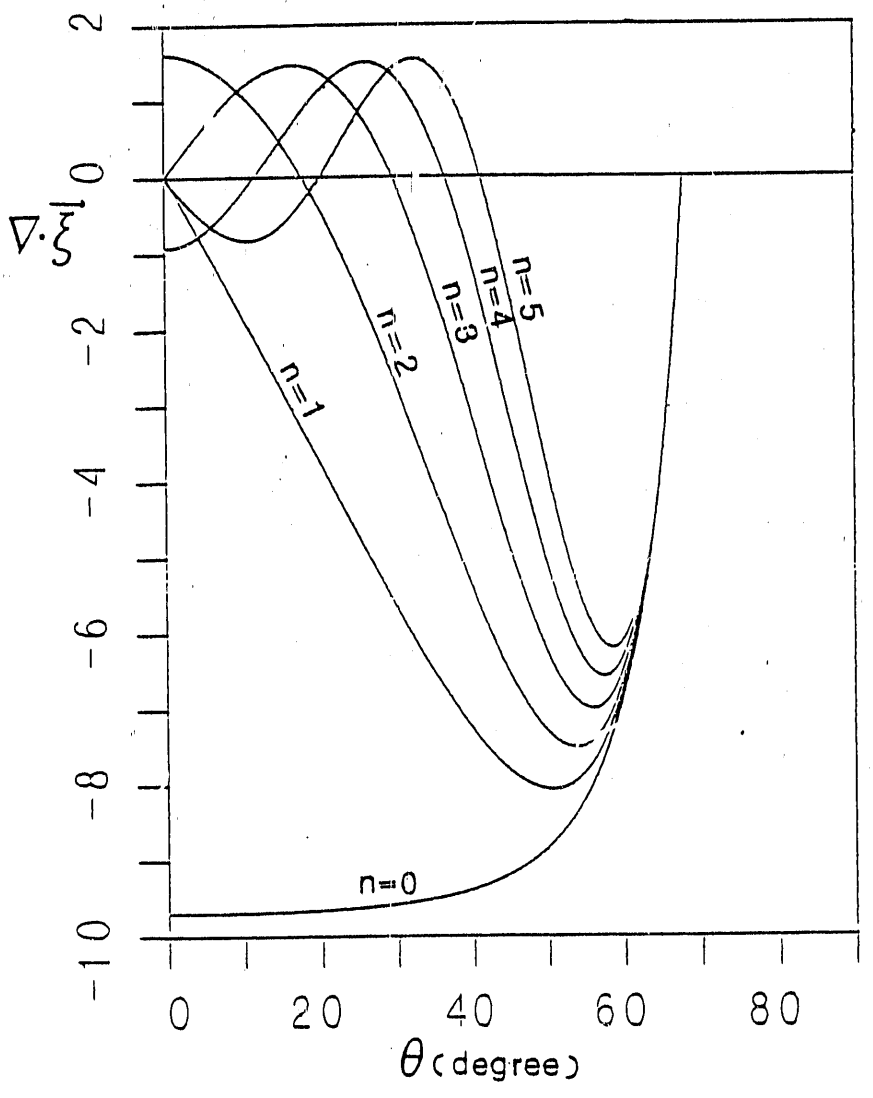

Fig. 2 SLOW MAGNETOSONIC WAVES (L=6)

EXTERNAL DISTRIBUTION IN ADDITION TO UC-420

Dr. F. Paoloni, Univ. of Wollongong, AUSTRALIA
Prof. M.H. Brennan, Univ. of Sydney, AUSTRALIA
Plasma Research Lab., Australian Nat. Univ., AUSTRALIA
Prof. I.R. Jones, Flinders Univ, AUSTRALIA
Prof. F. Cap, Inst. for Theoretical Physics, AUSTRIA
Prof. M. Heindler, Institut für Theoretische Physik, AUSTRIA
Prof. M. Goossens, Astronomisch Instituut, BELGIUM
Ecole Royale Militaire, Lab. de Phy. Plasmas, BELGIUM
Commission-European, DG. XII-Fusion Prog., BELGIUM
Prof. R. Boucqué, Rijksuniversiteit Gent, BELGIUM
Dr. P.H. Sakanaka, Instituto Fisica, BRAZIL
Instituto Nacional De Pesquisas Espaciais-INPE, BRAZIL
Documents Office, Atomic Energy of Canada Ltd., CANADA
Dr. M.P. Bachynski, MPB Technologies, Inc., CANADA
Dr. H.M. Skarsgard, Univ. of Saskatchewan, CANADA
Prof. J. Teichmann, Univ. of Montreal, CANADA
Prof. S.R. Sreenivasan, Univ. of Calgary, CANADA
Prof. T.W. Johnston, INRS-Energie, CANADA
Dr. R. Bolton, Centre canadien de fusion magnétique, CANADA
Dr. C.R. James,, Univ. of Alberta, CANADA
Dr. P. Lukác, Komenského Universzita, CZECHO-SLOVAKIA
The Librarian, Culham Laboratory, ENGLAND
Library, R61, Rutherford Appleton Laboratory, ENGLAND
Mrs. S.A. Hutchinson, JET Library, ENGLAND
Dr. S.C. Sharma, Univ. of South Pacific, FIJI ISLANDS
P. Mähönen, Univ. of Helsinki, FINLAND
Prof. M.N. Bussac, Ecole Polytechnique,, FRANCE
C. Mouttet, Lab. de Physique des Milieux Ionisés, FRANCE
J. Radet, CEN/CADARACHE - Bat 506, FRANCE
Prof. E. Economou, Univ. of Crete, GREECE
Ms. C. Rinni, Univ. of Ioannina, GREECE
Dr. T. Mual, Academy Bibliographic Ser., HONG KONG
Preprint Library, Hungarian Academy of Sci., HUNGARY
Dr. B. DasGupta, Saha Inst. of Nuclear Physics, INDIA
Dr. P. Kaw, Inst. for Plasma Research, INDIA
Dr. P. Rosenau, Israel Inst. of Technology, ISRAEL
Librarian, International Center for Theo Physics, ITALY
Miss C. De Palo, Associazione EURATOM-ENEA , ITALY
Dr. G. Grosso, Istituto di Fisica del Plasma, ITALY
Prof. G. Rostangni, Istituto Gas Ionizzati Del Cnr, ITALY
Dr. H. Yamato, Toshiba Res & Devel Center, JAPAN
Prof. I. Kawakami, Hiroshima Univ., JAPAN
Prof. K. Nishikawa, Hiroshima Univ., JAPAN
Director, Japan Atomic Energy Research Inst., JAPAN
Prof. S. Itoh, Kyushu Univ., JAPAN
Research Info. Ctr., National Instit. for Fusion Science, JAPAN
Prof. S. Tanaka, Kyoto Univ., JAPAN
Library, Kyoto Univ., JAPAN
Prof. N. Inoue, Univ. of Tokyo, JAPAN
Secretary, Plasma Section, Electrotechnical Lab., JAPAN
S. Mori, Technical Advisor, JAERI, JAPAN
Dr. O. Mitarai, Kumamoto Inst. of Technology, JAPAN
J. Hyeon-Sook, Korea Atomic Energy Research Inst., KOREA
D.I. Choi, The Korea Adv. Inst. of Sci. & Tech., KOREA
Prof. B.S. Liley, Univ. of Waikato, NEW ZEALAND
Inst of Physics, Chinese Acad Sci PEOPLE'S REP. OF CHINA
Library, Inst. of Plasma Physics, PEOPLE'S REP. OF CHINA
Tsinghua Univ. Library, PEOPLE'S REPUBLIC OF CHINA
Z. Li, S.W. Inst Physics, PEOPLE'S REPUBLIC OF CHINA
Prof. J.A.C. Cabral, Instituto Superior Tecnico, PORTUGAL
Dr. O. Petrus, AL I CUZA Univ., ROMANIA
Dr. J. de Villiers, Fusion Studies, AEC, S. AFRICA
Prof. M.A. Hellberg, Univ. of Natal, S. AFRICA
Prof. D.E. Kim, Pohang Inst. of Sci. & Tech., SO. KOREA
Prof. C.I.E.M.A.T, Fusion Division Library, SPAIN
Dr. L. Stenflo, Univ. of UMEA, SWEDEN
Library, Royal Inst. of Technology, SWEDEN
Prof. H. Wilhelmson, Chalmers Univ. of Tech., SWEDEN
Centre Phys. Des Plasmas, Ecole Polytech, SWITZERLAND
Bibliotheek, Inst. Voor Plasma-Fysica, THE NETHERLANDS
Asst. Prof. Dr. S. Cakir, Middle East Tech. Univ., TURKEY
Dr. V.A. Glukhikh,Sci. Res. Inst. Electrophys.I Apparatus, USSR
Dr. D.D. Ryutov, Siberian Branch of Academy of Sci., USSR
Dr. G.A. Eliseev, I.V. Kurchatov Inst., USSR
Librarian, The Ukr.SSR Academy of Sciences, USSR
Dr. L.M. Kovrizhnykh, Inst. of General Physics, USSR
Kernforschungsanlage GmbH, Zentralbibliothek, W. GERMANY
Bibliothek, Inst. Für Plasmaforschung, W. GERMANY
Prof. K. Schindler, Ruhr-Universität Bochum, W. GERMANY
Dr. F. Wagner, (ASDEX), Max-Planck-Institut, W. GERMANY
Librarian, Max-Planck-Institut, W. GERMANY
Prof. R.K. Janev, Inst. of Physics, YUGOSLAVIA

DATE
FILMED
3/16/92